Automotive Radar 4D Point Cloud Imaging

Ron Bartov
Electrical and Computer Engineering Departmet
Ben Gurion University
Beer Sheva, Israel
Email: ronbartov1@gmail.com

***Abstract*—This paper presents a study about a signal processing algorithm that enable high-fidelity four-dimensional (4D) sensing for autonomous driving, i.e, detecting the range, velocity, azimuth, and elevation of target scatters respect to the radar, using a 2D sparse multiple-input and multiple-output (MIMO) antenna array. The algorithm uses fast 2D-FFT digital beamforming (DBF), matrix completion (MC), and the correction of motion-induced phase by the switch delay of the time-division MIMO (TDM-MIMO) to calculate the azimuth and elevation of scatters. The result is a clear point-cloud image that can be used for automatic driving technology. While the presented method uses TDM-MIMO for maintaining orthogonality along all the transmit antennas, an additional technique will be proposed for maintaining the orthogonality by using Doppler Division Multiple Access (DDMA), which relies on the frequency domain. The proposed technique is validated through different automotive radar simulations.**

***Index Terms*— ADASs, DBF, FFT, TDM-MIMO radar, DDMA**

I. INTRODUCTION

In conjunction with lidar, cameras, ultrasonic sensors, and other technologies, automotive radar contributes to the development of ADASs, ensuring safer and more efficient driving experiences [1] [2]. Unlike some common sensors like lidar and cameras, mmWave radar is known for its ability to function reliably in various weather conditions, making it essential for autonomous driving. Currently, there are three kinds of automotive radar in ADASs, the long-range radar, the medium-range radar, and the short-range radar. Each of these radar types serves specific functions within ADASs, such as adaptive cruise control, blind spot detection, and parking assistance [2]. Notably, the 77GHz automotive radar has gained prominence due to its advantages in performance and functionality. The frequency modulated continuous wave (FMCW) radar technology is widely employed in automotive radar systems. It offers convenient capabilities for measuring range, velocity, and angle concerning radar targets. Signal processing in FMCW radar involves several critical stages, including dechirping, moving target indication (MTI), moving target detection (MTD), and constant false alarm ratio (CFAR).

The TDM-MIMO is commonly used in the automotive radar product. However, the most automotive radar products only provide the velocity, range, and azimuth, and cannot measure the height information, which is essential to the ADASs. To address this limitation, paper [3] introduces a novel approach to design a 2D sparse planar array capable of estimating both azimuth and elevation angles of radar targets.

The authors propose a structured MC algorithm to address scenarios where entire columns and rows of data may be missing, and discuss how this approach differs from previous work that employed Hankel matrices to enhance angle resolution in sparse antenna arrays [4]. In contrast to earlier methods, their solution scheme aims to achieve 4D automotive radar imaging by constructing a 2D hybrid sparse array. This innovation is expected to conserve hardware resources and reduce storage memory requirements, offering significant benefits for automotive radar technology.

II. THE SIGNAL PROCESSING ALGRORITHM OF THE 1D AUTOMATIVE RADAR

The article considers the use of a sawtooth wave as the modulation waveform for Frequency Modulated Continuous Wave (FMCW) radar. This sawtooth waveform has specific characteristics: it has a chirp duration represented as T_r, a modulation bandwidth denoted as B, and a modulation slope known as K_r. Fig.1 illustrate the radar echo model, where the blue line denotes the transmitted signal with the center frequency f_c, and the red line denotes the echo signal with the time delay and the doppler frequency.

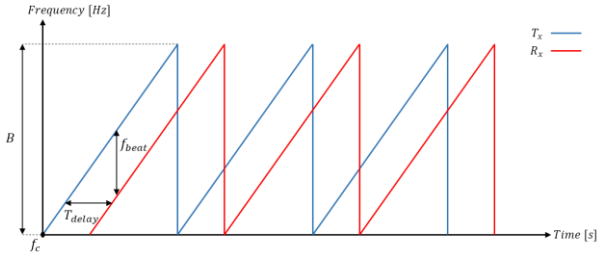

Fig. 1: Frequency modulated continuous wave (FMCW).

A. FMCW Radar Transceiver Model Derivation

The general schematic of the FMCW radar transceiver can be shown in Fig.2.

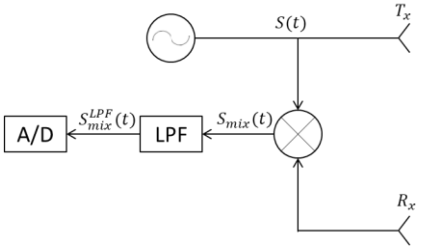

Fig. 2: General schematics of FMCW radar.

Assuming the transmitted signal has the following form

$$S_t(t) = \cos\left(2\pi\left(f_c t + \frac{K_r t^2}{2}\right)\right) \tag{1}$$

where $K_r = \frac{B}{T_r}$ and t is the fast time direction, then the echo signal can be shown as

$$S_r(t) = \sum_{i=1}^{K} \alpha_i \cdot \cos\left(2\pi\left(f_c(t-\tau_i) + \frac{K_r(t-\tau_i(n))^2}{2}\right)\right) \tag{2}$$

Where K denotes the number of scatters within the main beam, α_i denotes the i_{th} scattered signal intensity, and τ_i denotes the delay time due to the range between the radar and scatters. Within each chirp, the target is assumed stationary, but its position is changing from chirp to chirp. The change in the target's position between chirps can be related to its velocity, where this velocity is assumed constant for the duration of n chirps, hence, the time delay can be denoted as

$$\tau_i(n) = \frac{2(R_i + v_i(nT_r + t_s))}{c} \tag{3}$$

Where R_i represents the range of the object from the radar, v_i the velocity of the object, t_s the sampling period and c the propagation velocity of the electromagnetic wave in space. Next, by multiply the transmitting signal and the receiving echo signal and applying quadrature sampling on the result, the baseband mixed signal can be obtained, as shown in equation (4).

$$\begin{aligned} S_{mix}(t_s, nT_r) &= S_t(t)S_r(t)|_{sampled} \\ &\approx \sum_{i=1}^{K} \alpha_i \exp\left(j2\pi\left(\frac{2K_r}{c}(R_i + v_i nT_r)t_s \right.\right. \\ &\left.\left. + \frac{2v_i nT_r}{\lambda} + \frac{2f_c R_i}{c}\right)\right) \end{aligned} \tag{4}$$

Where $\lambda = \frac{c}{f_c}$ is the wavelength.

B. Basebamd Sampled Mixed Signal Expression for Specific Transmitter and Receiver Locations

Assume we have M_t transmitters and N_r receivers, and the spacing between adjacent transmitters and receivers are d_t and d_r respectively. If the relation $d_t = N_r d_r$ holds, then the baseband mixed signal received by the n_k receiver element while the transmission was from the m_k transmitter element, after quadrature sampling, can be expressed as

$$\begin{aligned} s(t_s, nT_r, m_k, n_k) = &\sum_{i=1}^{K} \alpha_i \exp\left(j2\pi\left(\frac{2K_r R i t_s}{c} + \frac{2v_i nT_r}{\lambda}\right)\right) \\ &\cdot \exp\left(\frac{j2\pi(m_k d_t + n_k d_r)sin\theta_i}{\lambda}\right) \\ &\cdot \exp\left(j\frac{4\pi v_i}{\lambda}T_k(m_k - 1)\right) \\ &\cdot \exp\left(j\frac{4\pi R_i}{\lambda}\right) \end{aligned} \tag{5}$$

While the expression also considers the phase error caused by the switch delay and the velocity of the target.

Note that the phase $\exp\left(j\frac{4\pi R_i}{\lambda}\right)$ can be compensated for every doppler bins [5].

III. 2D ANTENNA ARRAY SIGNAL PROCESSING

In paper [3] the authors use TDM-MIMO, a widely used technique, which often employed to enhance the size of the antenna array and conserve transceiver channels. If the aperture of the receiver array will be $(N_{r1} - 1)d_r \times (N_{r1} - 1)d_r$ and the aperture of the transmitter array will be $(M_{t1} - 1)d_t \times (M_{t1} - 1)d_t$, then the aperture of the virtual will be $M_{t1}N_{r1}d_r \times M_{t1}N_{r1}d_r$. Fig. 3 illustrates the configuration of a 2D TDM-MIMO system and the concept of a virtual antenna array.

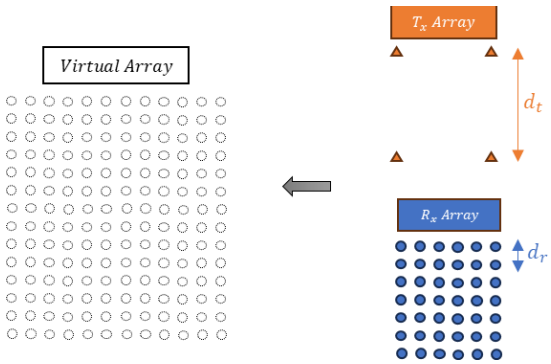

Fig. 3: TDM MIMO radar configuration, where the transmit array is 2x2 and the receive array is 7x7.

A. Virtual Array Steering Vector

The steering vector of the virtual array describes how signals are received or transmitted by the array elements for different directions or angles. It helps characterize the array's response to incoming signals. Assume we denote the position coordinate of the k-th receiver and k-th transmitter in the sparse array as (x_{rk}, y_{rk}) and (x_{tk}, y_{tk}) respectively, then the steering vectors of the receiver and transmitter arrays can be expressed by equations (6) and (7).

$$a_r(x_{rk}, y_{rk}) = \exp\left(j2\pi d_r \frac{x_{rk}cos\varphi_i sin\theta_i + y_{rk}cos\theta_i}{\lambda}\right) \tag{6}$$

$$a_t(x_{rk}, y_{rk}) = \exp\left(j2\pi d_t \frac{x_{tk}cos\varphi_i sin\theta_i + y_{tk}cos\theta_i}{\lambda}\right) \tag{7}$$

By using the Kronecker product, the steering vector of the virtual array can be expressed by equation (8)

$$\boldsymbol{a_{vir}} = \boldsymbol{a_t} \otimes \boldsymbol{a_r} \tag{8}$$

Now, equation (5) can be updated to

$$\begin{aligned} s(t_s, nT_r, m_k, n_k) = &\sum_{i=1}^{K} \alpha_i \exp\left(j2\pi\left(\frac{2K_r R i t_s}{c} + \frac{2v_i nT_r}{\lambda}\right)\right) \\ &\cdot \exp\left(j\frac{4\pi v_i}{\lambda}T_k(m_k - 1)\right) \\ &\cdot a_{vir}(m_k, n_k) \cdot \exp\left(j\frac{4\pi R_i}{\lambda}\right) \end{aligned} \tag{9}$$

B. The Snapshot Matrix

The snapshot matrix represents the collected data over a specific time, typically capturing multiple samples or snapshots of received signals. Over a short time interval, the signals received by each antenna element are sampled at discrete time points. These time points represent the snapshots in time. The collected data is organized into a matrix form, where each row corresponds to a specific antenna element, and each column represents a snapshot in time. To deal with the whole column data missing in the snapshot matrix, the SIALM method is suggested. This

method is based on the rearranging of the snapshot matrix as two-fold Hankel matrix [6].

C. Calculating the Range

To calculate the range of a target, the MTD process examines the phase shift of the radar signals in the snapshot matrix. The phase shift is caused by the time delay between the transmitted signal and the received echo and by comparing the phase of the received signal in different snapshots, the range to a target can be estimated as

$$R = \frac{change\ in\ phase}{2\pi} \cdot \frac{c}{f_c} \tag{10}$$

D. Calculating Velocity

The velocity of a target is determined by examining the Doppler shift of the radar echoes in the snapshot matrix. The Doppler frequency shift is calculated as the difference in frequency between consecutive snapshots and the velocity of the target can be calculated as

$$v = \frac{Doppler\ Shift}{2f_c t_s} \tag{11}$$

E. Calculating Azimuth and Elevation

By performing the 2D-FFT on the snapshot matrix, a spectral representation of the received can be obtained. To estimate the azimuth and elevation, a peak detection technique in the 2D spectrum must be perform, and the coordinates of the detected peaks will be corresponded to the estimated azimuth and elevation angles of the targets. For the mentioned configuration, this can be express as

$$\phi = \arcsin\left(\frac{\lambda_k}{d_r M_{t1} N_{r1}}\right), k \in [0,1,\dots,M_{t1}N_{r1}-1] \tag{12}$$

$$\theta = \arccos\left(\frac{\lambda_k}{d_r M_{t1} N_{r1}}\right), k \in [0,1,\dots,M_{t1}N_{r1}-1] \tag{13}$$

And the angle φ in the steering vectors equations can be express as

$$\varphi = \arccos\left(\frac{sin\phi}{sin\theta}\right) \tag{14}$$

IV. DDMA BASED AUTOMOTIVE MIMO RADAR

A. Orthogonality Using Time Domain

An essential characteristic of any MIMO radar implementation is a waveform that maintains orthogonality along all the transmitting antennas. This orthogonality is often realized by encoding the transmitted waveforms in time, frequency, or code domains. Maintaining this orthogonality across the transmit antennas is essential in order to assemble the virtual array used by the MIMO radar. In the presented article, the time division multiple access (TDMA) technique has been applied to obtain the MTD, which is then used for estimating the azimuth and elevation. However, this technique suffers from the transmit energy loss, and as a result the parameter estimation performance degradation when the number of transmit elements increases [7].

B. Orthogonality Using Frequency Domain

To tackle the problem of energy loss and estimation performance degradation while implementing orthogonality in time domain, a transmit Doppler Division Multiple Access (DDMA) approach is proposed and will be validate through simulations in next sections. DDMA maintains orthogonality in the frequency domain by shifting the waveforms transmitted by each transmitting antenna in Doppler [8]. The motivation of this approach is to separate transmit signals from the M_t transmit antennas into M_t Doppler frequency sub bands at the receiver. This is realized by DDMA MIMO weights which modulate each transmit antenna's signal into its own Doppler frequency sub band. The DDMA approach can fully take advantage of the transmission capabilities of the transmit array as all transmit elements can emit simultaneously at any time. The waveform diversity is achieved at the cost of a higher-level Pulse Repetition Frequency (PRF) tolerance, and to meet the requirements on the maximum unambiguous velocity, the system Pulse Repetition Interval (PRI) needs to be decreased, what makes DDMA technique to be suitable only for Short Range Radar (SRR) applications. Because the presented article is focusing on ADAS, then the DDMA method can be considered as valid.

V. EXPERIMENTS AND SIMULATIONS

In this section, a detailed MATLAB simulation for automotive imaging with 2D MIMO radar using DDMA technique will be explained. The simulation includes modeling 2D MIMO radar transceiver, defining transmit and receive arrays, defining MIMO DDMA waveform and generating a range-doppler detection map. In order to provide a clear explanation about the simulation, each step will be described in detail, including its programming aspect.

A. Model a MIMO Radar Transceiver

To create a radar transceiver model for simulating FMCW automotive MIMO radar, a 'radarTransceiver' object was defined. The properties of the radar transceiver object can be found in Table 1.

Symbol	Parameter Description	Value
f_c	carrier frequency	$77GHz$
λ	wavelength	$3.9mm$
$rgRes$	range resolution	$0.5m$
$rgMax$	maximum detection range	$150m$
$N_{tx} \times N_{tx}$	number of transmitters	$4\ (2 \times 2)$
$N_{rx} \times N_{rx}$	number of receivers	$49\ (7 \times 7)$
$sweepBW$	bandwidth of FMCW wave	$750MHz$
N_{cp}	number of chirps	250
F_s	sampling frequency	$100MHz$
d_r	interval between adjacent receivers	$\lambda/2$
d_t	interval between adjacent transmitters	$N_{rx} \times d_r$
$sweepTime$	duration of one chirp	$20\mu s$

Table 1: Radar transceiver simulation parameters.

The architecture of the transmit and receive arrays was chosen to have a 2D rectangular shape and with isotropic

antenna elements. The configurations of the transmit array, receive array and the virtual array can be seen in Fig. 4.

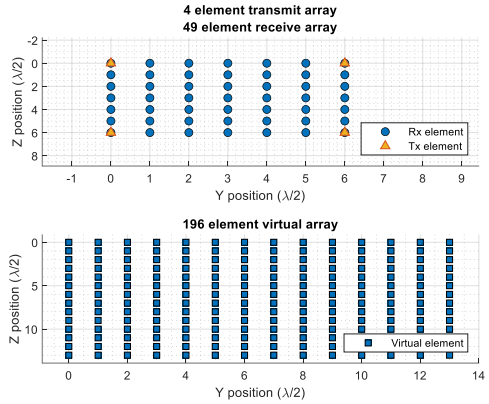

Fig. 4: Simulation transmit and receive arrays configurations.

B. Calculating Azimuth and Elevation Resolution

By using the transmit and receive arrays properties, the azimuth and elevation resolutions were calculated. In the context of a 2D MIMO transceiver system, azimuth and elevation resolution refer to the system's ability to distinguish between closely spaced targets or objects in the horizontal and vertical dimensions, and it calculated by obtaining the $-3dB$ bandwidth from the azimuth and elevation directivities pattern of the virtual array. The directivity patterns and the resolutions values can be seen in Fig. 5 and Fig. 6.

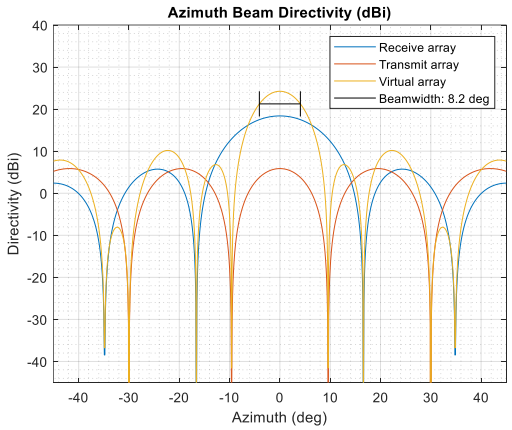

Fig. 5: Virtual array azimuth beam directivity.

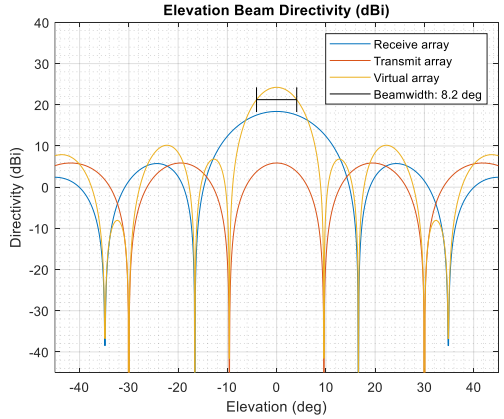

Fig. 6: Virtual array elevation beam directivity.

C. Define MIMO DDMA Waveform

For each transmit antenna element, the same FMCW waveform was assigned, but with a unique offset in Doppler. The Doppler offsets were generated uniformly across the Doppler space for the 4 transmit elements (according to the configuration in Table 1) and 2 additional virtual antennas, which will use for preventing a reduction in the maximum ambiguous velocity of the MIMO radar. Fig. 7 presents the Doppler offsets, with Doppler represented in degrees on the unit circle. This representation is achieved by normalizing the Doppler shift frequencies from $[-\frac{PRF}{2}, \frac{PRF}{2}]$ to the range $[-\pi, \pi]$ using $\frac{PRF}{2\pi}$.

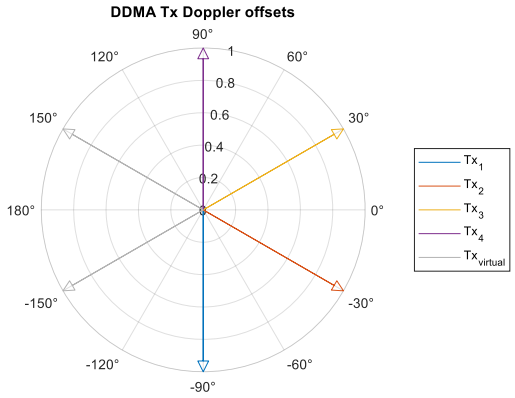

Fig. 7: Doppler frequencies offset for the transmit elements.

D. Simulate Radar Data Cube

In this radar simulation, the data cube refers to the three-dimensional data structure that represents radar measurements over time, across range, and across the Doppler dimension. To Carry out a simulation that will be as close as possible to a real autonomous driving scenario, two driving scenarios were designed using 'MATLAB Driving Scenario Designer', and their configurations can be found in Table 2 and Table 3.

Description	Type/Class ID	Speed	Path/ Direction
road	road	static	vertical
road1	road	static	horizontal
egoVehicle	vehicle: class ID 1	static	static
car1	actor: class ID 1	30 m/s	horizontal
bicycle	actor: class ID 3	15 m/s	horizontal

Table 2: Configuration for the first driving scenario simulation.

Description	Type/Class ID	Speed	Path/ Direction
road	road	static	vertical
egoVehicle	vehicle: class ID 1	static	static
car1	actor: class ID 1	35 m/s	vertical
car2	actor: class ID 3	40 m/s	vertical

Table 3: Configuration for the second driving scenario simulation.

In both simulations configurations, the radar object is attached to a static car with field of view of 85° in the azimuth axis and 25° in the elevation axis, while the object around it are moving according to a defined pattern. The different scenarios visualizations can be seen in Fig. 8 and Fig. 9.

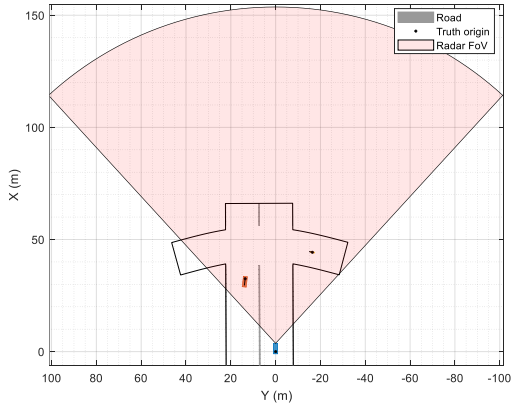

Fig. 8: Snapshot from the first driving scenario, containing the main vehicle with the radar, and additional vehicle and bicycle as targets.

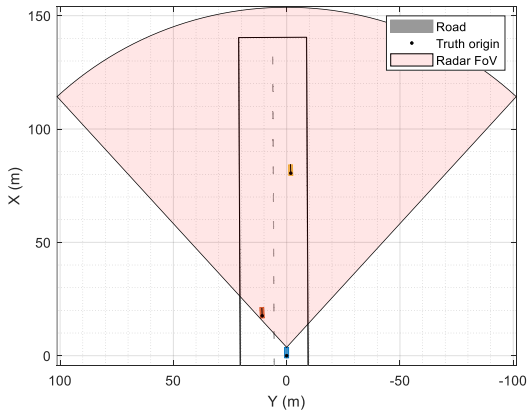

Fig. 9: Snapshot from the second driving scenario, containing the main vehicle with the radar and two additional vehicles as targets.

E. Generate Range-Doppler Map

A 'phased.RangeDopplerResponse' object was defined in order to extract the range and doppler bins from the first and third dimensions of the data cube by applying 2D-FFT on it. Then, by defining a 'phased.CFARDetector' object and applying it on the range doppler response, the location of the targets were detected. Fig. 10 shows the detection results from one of the receive elements and for the first scenario.

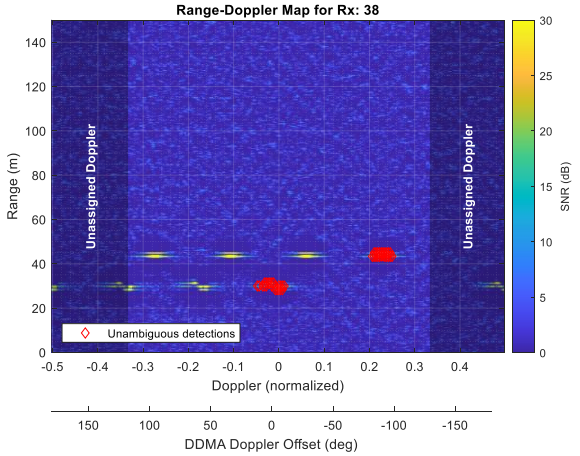

Fig. 10: Range-Doppler map correspond to one of the receivers. The detected targets are colored red.

As can be seen in Fig. 10, there are four returns modulated in Doppler at the same range for each target corresponding to the four Doppler offsets applied across each of the four transmit elements. A gap in Doppler between the first and last transmit element's target returns exists because of the virtual transmit antennas used to compute the DDMA Doppler offsets [8].

F. Remove Doppler Ambiguities

Doppler ambiguity arises when multiple objects or targets have similar Doppler shifts or velocities, making it difficult to distinguish between them. In radar applications, this ambiguity can occur because the radar measures the change in frequency of the returned signal (Doppler shift), but it may not always be clear which target or object is responsible for a particular Doppler shift. For removbing Doppler ambiguities, a matched filter was designed to identify the location of the first transmit element for each of the target returns locations identified by the CFAR detector object. Fig. 11 and Fig. 12 shows the matched filter coefficients and the Range-Doppler detections after removing the DDMA Doppler offset applied to the first transmit element.

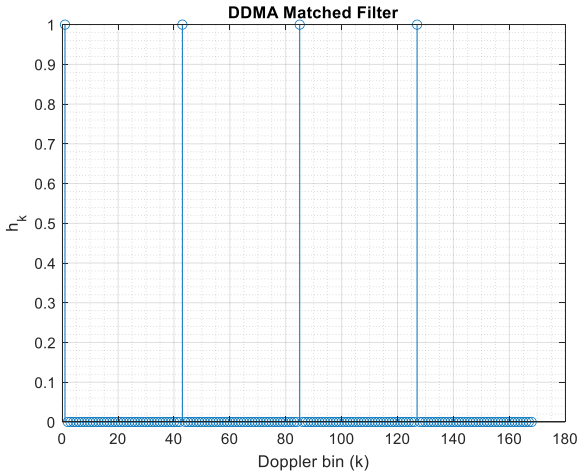

Fig. 11: DDMA matched filter coefficients.

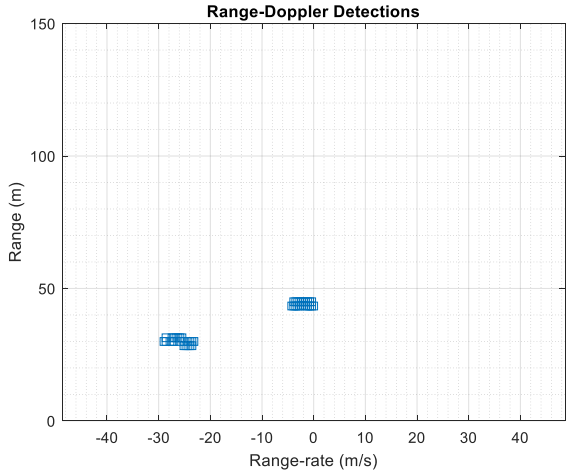

Fig. 12: Range-Doppler map after removing the DDMA Doppler offset applied to the first transmit element.

CONCLUSIONS

In this paper, a 4D sensing technique for autonomous driving using 2D TDM-MIMO and signal processing algorithms were presented and studied. To tackle the problem of transmission energy loss, an additional transmitting method was proposed, based on orthogonality implementation in the frequency domain instead of the time domain. Due to this fact, the proposed method makes it possible to transmit at the same time from all transmitters. We note that due to the limitation on the system PRI, the proposed method is more suitable for SRR application, but in the context of ADAS, which the main topic that studied through this paper, it can be consider as valid and hence as a possible improvement for the studied article.

REFERENCES

[1] S. Sun and A. P. Petropulu, "A sparse linear array approach in automotive radars using matrix completion," in ICASSP 2020 - 2020 IEEE International Conference on Acoustics, Speech and Signal Processing (ICASSP), 2020, pp. 8614–8618.

[2] S. M. Patole, M. Torlak, D. Wang, and M. Ali, "Automotive radars: A review of signal processing techniques," IEEE Signal Processing Magazine, vol. 34, no. 2, pp. 22–35, 2017.

[3] J. Ding, W. Ma, Z. Wang, H. Kang and M. Wang, "Automotive radar 4D Point-cloud Imaging with 2D Sparse Array," 2021 CIE International Conference on Radar (Radar), Haikou, Hainan, China, 2021, pp. 2838-2842, doi: 10.1109/Radar53847.2021.10028211.

[4] L. T. Nguyen, J. Kim, and B. Shim, "Low-rank matrix completion: A contemporary survey," IEEE Access, vol. PP, no. 99, pp. 1–1, 2019.

[5] S. Haefner and R. Thoma, "Compensation of motion-induced phase errors and enhancement of doppler unambiguity in tdm-mimo systems by model-based estimation," IEEE Sensors Letters, vol. PP, no. 99, pp. 1–1, 2020.

[6] Y. Chen and Y. Chi, "Robust spectral compressed sensing via structured matrix completion," IEEE Transactions on Information Theory, vol. 60, no. 10, pp. 6576–6601, 2014.

[7] F. Jansen, "Automotive radar Doppler division MIMO with velocity ambiguity resolving capabilities," in 2019 16th European Radar Conference (EuRAD), Paris, France, Oct. 2019, pp. 245–248.

[8] F. Xu, S. A. Vorobyov, and F. Yang, "Transmit beamspace DDMA based automotive MIMO radar," IEEE Trans. Veh. Technol., vol. 71, no. 2, pp. 1669–1684, Feb. 2022.